

# From the Kondo Regime to the Mixed-Valence Regime in a Single-Electron Transistor

D. Goldhaber-Gordon\*, J. Göres, and M.A. Kastner  
*Department of Physics, Massachusetts Institute of Technology  
 Cambridge, MA 02139*

Hadas Shtrikman, D. Mahalu, and U. Meirav  
*Braun Center for Submicron Research  
 Weizmann Institute of Science  
 Rehovot, Israel 76100  
 (February 1, 2008)*

We demonstrate that the conductance through a single-electron transistor at low temperature is in quantitative agreement with predictions of the equilibrium Anderson model. When an unpaired electron is localized within the transistor, the Kondo effect is observed. Tuning the unpaired electron's energy toward the Fermi level in nearby leads produces a cross-over between the Kondo and mixed-valence regimes of the Anderson model.

PACS 75.20.Hr, 73.23.Hk, 72.15.Qm, 73.23.-b

The effect of magnetic impurities on metals — the Kondo effect — has been studied for half a century, and enjoys continued relevance today in attempts to understand heavy-fermion materials and high- $T_c$  superconductors. Yet it has not been possible to experimentally test the richly varied behavior predicted theoretically. The theory depends on several parameters whose values are not independently tunable for impurities in a metal, and are often not even *a priori* known. On the other hand, it has been predicted [1–5] that a single-electron transistor (SET) should be described by the Anderson impurity model, and hence should also exhibit the Kondo effect. An SET contains a very small droplet of localized electrons, analogous to an impurity, strongly coupled to conducting leads, analogous to the host metal. We have recently shown that when the number of electrons in the droplet is odd, and hence one electron is unpaired, the SET exhibits the Kondo effect [6] in electronic transport. This observation has since been confirmed [7,8] with additional quantitative detail. As we show in this Letter, in SET experiments one can tune the important parameters and test predictions of the Anderson model that cannot be tested in bulk metals.

In our SET, a droplet of about 50 electrons is separated from two conducting leads by tunnel barriers. A set of electrodes (Fig. 1(a)), on the surface of a GaAs/AlGaAs heterostructure which contains a two-dimensional electron gas (2DEG), is used to confine the electrons and create the tunnel barriers. The 2DEG is depleted beneath the electrodes, and the narrow constrictions between electrodes form the tunnel barriers. Details of the device fabrication and structure are given elsewhere [6].

In the Anderson model, the SET is approximated as a single localized state, coupled by tunneling to two electron reservoirs. The state can be occupied by  $n_d = 0, 1$ , or 2 electrons with opposite spin; couplings to all other filled and empty states of the droplet are neglected.

Adding the first electron takes an energy  $\epsilon_0$  referenced to the Fermi level in the leads, but the second electron requires  $\epsilon_0 + U$ , where the extra charging energy  $U$  ( $1.9 \pm 0.05$  meV in our SET) results from Coulomb repulsion. In the diagram of Fig. 1(b),  $\epsilon_0 < 0$ , but  $\epsilon_0 + U > 0$ , so there is one electron in the orbital. However, this electron can tunnel into the leads, with rate  $\Gamma/h$ , leading to Lorentzian broadening of the localized-state energies with full width at half maximum (FWHM)  $\Gamma$ . The energy  $\epsilon_0$  can be raised by increasing the negative voltage  $V_g$  on a nearby electrode (the middle left “plunger gate” electrode in Fig. 1(a)) and  $\Gamma$  can be tuned by adjusting the voltages on the gates that form the constrictions. Two other important energies (not shown) are the spacing between quantized single-particle levels  $\Delta\epsilon \approx 400 \mu\text{eV}$ , and the thermal broadening of the Fermi level in the leads  $kT = 8 - 350 \mu\text{eV}$ . The Kondo temperature  $T_K$  is a new, many-body energy scale that emerges for a singly-occupied Anderson impurity [9]. It is essentially the binding energy of the spin singlet formed between the localized, unpaired electron and electrons in the surrounding reservoirs;  $kT_K \approx 4 - 250 \mu\text{eV}$  in our SET, depending on the other tunable parameters.

The conductance  $G$  of an SET is analogous to the resistivity  $\rho$  of a bulk Kondo system. Although one thinks of the increase in resistivity at low  $T$  as the hallmark of the Kondo effect, transport properties have proven more difficult to calculate than thermodynamic properties. For  $T \ll T_K$ ,  $\rho$  is theoretically and experimentally known to equal  $\rho_0 - cT^2$  (Fermi liquid behavior) [10] and for  $T_K < T < 10 T_K$ ,  $\rho$  is roughly logarithmic in  $T$  [11,12], but the crossover region has only recently been successfully treated [13].

Furthermore, the Anderson model has several interesting regimes parametrized by  $\tilde{\epsilon}_0 \equiv \epsilon_0/\Gamma$ : the Kondo regime  $\tilde{\epsilon}_0 \ll -0.5$ , the mixed-valence regime  $-0.5 \lesssim \tilde{\epsilon}_0 \lesssim 0$ , and the empty orbital regime  $\tilde{\epsilon}_0 \gtrsim 0$ , each of which has dif-

ferent transport properties. The Kondo regime describes many systems of dilute magnetic impurities in metals, while the mixed-valence regime provides some understanding of heavy-fermion compounds [14–16]. We know of no material described by the empty orbital regime. Though conductance through an SET normalized to its zero-temperature value  $\tilde{G}(T) \equiv G(T/T_K)/G_0$  is expected to be universal in the Kondo regime, where the only small energy scale is  $T_K$ , it should change as  $\tilde{\epsilon}_0 \rightarrow 0$  (the mixed-valence regime), where  $T_K$  and  $\Gamma$  become comparable [13]. The great advantage of the SET is that  $\epsilon_0$  can be tuned by varying  $V_g$  to test the predictions for all regimes in one and the same system.

As  $V_g$  is varied, the conductance of an SET undergoes oscillations caused by what is usually called the Coulomb blockade. Current flow is possible in this picture only when two charge states of the droplet are degenerate, i.e.  $\epsilon_0 = 0$  or  $\epsilon_0 + U = 0$ , marked by vertical dashed lines in Fig. 2 as determined by the analysis of Fig. 5. The conductance between these dashed lines is expected to be very small. However, in this range the charge state of the site is odd, as portrayed in Fig. 1, and the Kondo effect allows additional current flow. Strikingly, at low temperature (dots, 100 mK and triangles, 800 mK), the conductance maxima do not even occur at  $\epsilon_0 = 0$  and  $\epsilon_0 + U = 0$  — the Kondo effect makes the off-resonant conductance even larger than the conductance at the charge-degeneracy point [4]. Raising the temperature suppresses the Kondo effect, causing the peaks to approach the positions of the bare resonances.

The inset of Fig. 2 shows how  $\Gamma$  is determined: For  $T \geq \Gamma/2$ , the conductance peak is well-described by the convolution of a Lorentzian of FWHM  $\Gamma$  with the derivative of a Fermi-Dirac function (FWHM  $3.52kT$ ). This convolution has a FWHM  $0.78\Gamma + 3.52kT$ , so extrapolating the experimentally-measured linear dependence back to  $T = 0$  gives  $\Gamma = 295 \pm 20 \mu\text{eV}$ .

When the energy of the localized state is far below the Fermi level ( $\tilde{\epsilon}_0 \ll -1$ ), scaling theory predicts that  $T_K$  depends exponentially on the depth of that level [17]:

$$T_K = \frac{\sqrt{\Gamma U}}{2} e^{\pi \epsilon_0 (\epsilon_0 + U) / \Gamma U}. \quad (1)$$

Note that, because  $U$  is finite,  $\log T_K$  is quadratic in  $\epsilon_0$ . This strong dependence on  $\epsilon_0$  causes the Kondo-enhanced conductance to persist to higher temperatures near  $\epsilon_0 = 0$  (and near  $\epsilon_0 = -U$ , by particle-hole symmetry) than in-between. In fact, at  $T = 0$  the conductance should sustain its maximum value all the way between the two observed peaks in Fig. 2 [1,2,6] (see Fig. 5(b) for expected  $G(\tilde{\epsilon}_0)$  at  $T = 0$ ), but in the valley even our  $T_{\text{base}} \simeq 100 \text{ mK} > T_K \approx 40 \text{ mK}$ .

Figure 3(a) shows that, for fixed  $\tilde{\epsilon}_0$  in the Kondo regime,  $G \sim -\log(T)$  over as much as an order of magnitude in temperature, beginning at  $T_{\text{base}}$ . Thermal fluctuations in localized state occupancy cut off the  $\log(T)$  con-

ductance for  $kT \gtrsim |\epsilon_0|/4$ , consistent with simulations of thermally-broadened Lorentzian resonances. As  $\tilde{\epsilon}_0 \rightarrow 0$  (Fig. 3(b)),  $T_K$  increases, as evinced by the saturation of the conductance at low temperature.

To fit the experimental data for each  $\epsilon_0$  we use the empirical form

$$G(T) = G_0 \left( \frac{T_K'^2}{T^2 + T_K'^2} \right)^s, \quad (2)$$

where  $T_K'$  is taken to equal  $T_K/\sqrt{2^{1/s}-1}$  so that  $G(T_K) = G_0/2$ . For the appropriate choice of  $s$ , which determines the steepness of the conductance drop with increasing temperature, this form provides a good fit to numerical renormalization group results [13] for the Kondo, mixed-valence, and empty orbital regimes, giving the correct Kondo temperature in each case. The parameter  $s$  is left unconstrained in the fit to our data, but its fit value is nearly constant at  $0.20 \pm 0.01$  in the Kondo regime, while as expected it varies rapidly as we approach the mixed-valence regime (Figure 3(b)). The expected value of  $s$  in the Kondo regime depends on the spin of the impurity:  $s = 0.22 \pm 0.01$  for  $\sigma = 1/2$ .

Using the values of  $G_0$  and  $T_K$  extracted in this way we confirm that  $\tilde{G}$  is universal in the Kondo regime. Figure 4 shows  $\tilde{G}(\tilde{T})$  for data like those of Figure 3 for various values of  $\tilde{\epsilon}_0 \sim -1$  (on the left peaks of Fig. 2). We have also included data from the same SET, but with  $\Gamma$  reduced by 25% by adjusting the point-contact voltages. The data agree well with numerical renormalization group calculations by Costi and Hewson (solid line) [13]. In the mixed-valence regime it is difficult to make a quantitative comparison between theoretical predictions and our experiment. Qualitatively, in both calculation and experiment,  $\tilde{G}(\tilde{T})$  exhibits a sharper crossover between constant conductance at low temperature and logarithmic dependence at higher temperature in the mixed-valence regime than in the Kondo regime (see Fig. 4) [13].

In Figure 5(a), we plot  $T_K(\tilde{\epsilon}_0)$  extracted from our fits, along with the theoretical prediction (Eq. 1) for the Kondo regime. The value of  $\Gamma = 280 \pm 10 \mu\text{eV}$  extracted is in good agreement with the value  $\Gamma = 295 \pm 20 \mu\text{eV}$  determined as illustrated in Fig. 2 (inset). The prefactor is approximately three times larger than  $\sqrt{\Gamma U}/2$ , which must be considered good agreement given the simplifying assumptions in the calculations and the sensitivity to the value of the exponent [19].

$G_0$  is predicted to vary with the site occupancy  $n_d$ , and hence also with  $\tilde{\epsilon}_0$ , according to the Friedel sum rule

$$G_0(n_d) = G_{\text{max}} \sin^2 \left( \frac{\pi}{2} n_d \right), \quad (3)$$

where  $G_{\text{max}}$  is the unitary limit of transmission:  $2e^2/h$  if the two barriers are symmetric, less if they are asymmetric. For small  $|\tilde{\epsilon}_0|$ ,  $T_K \gg T_{\text{base}}$ , so we can directly measure the value of  $G_0$ . Even when  $T_K$  is not  $\gg T_{\text{base}}$ ,

we can still extract the value of  $G_0$  from our fit. In Figure 5(b), we compare the combined results of both these methods with  $G_0(\tilde{\epsilon}_0)$  inferred from a non-crossing approximation (NCA) calculation [4] of  $n_d(\tilde{\epsilon}_0)$  according to Equation 3. The agreement is excellent except outside the left peak, where experimentally the conductance does not go to zero even at zero temperature (see Fig. 2) [21].

We have demonstrated quantitative agreement between transport measurements on an SET and calculations for a spin-1/2 Anderson impurity. The SET allows us to both accurately measure and vary  $\Gamma$  and  $\epsilon_0$ , and to observe their effect on  $T_K$  and  $G_0$ . We have also observed the cross-over between the Kondo and mixed-valence regimes.

We acknowledge fruitful discussions with David Abusch-Magder, Igor Aleiner, Ray Ashoori, Gene Bickers, Daniel Cox, Leonid Glazman, Selman Hershfield, Wataru Izumida, Steven Kivelson, Leo Kouwenhoven, Patrick Lee, Leonid Levitov, Avraham Schiller, Chandradevar Varma, and especially Ned Wingreen, Yigal Meir, and Theo Costi. Theo Costi, Wataru Izumida, and Ned Wingreen generously provided data from their prior calculations. D. G.-G. thanks the Hertz Foundation, and J. G. thanks NEC, for graduate fellowship support. This work was supported by the US Army Research Office Joint Services Electronics Program under contract DAAG 55-98-1-0080, by the US Army Research Office under contract DAAG 55-98-1-0138, and by the MRSEC Program of the National Science Foundation under Award No. DMR94-00334.

---

\* *davidg@mit.edu*. Also at Weizmann Institute.

- [1] T. K. Ng and P. A. Lee, Physical Review Letters **61**, 1768 (1988).
- [2] L. I. Glazman and M. E. Raikh, JETP Letters **47**, 452 (1988).
- [3] Y. Meir, N. S. Wingreen, and P. A. Lee, Physical Review Letters **70**, 2601 (1993).
- [4] N. S. Wingreen and Y. Meir, Physical Review B **49**, 11040 (1994).
- [5] W. Izumida, O. Sakai, and Y. Shimizu, LANL archives **cond-mat** /9805067 (1998).
- [6] D. Goldhaber-Gordon *et al.*, Nature **391**, 156 (1998).
- [7] S. M. Cronenwett, T. H. Oosterkamp, and L. P. Kouwenhoven, LANL archives **cond-mat** /9804211 (1998).
- [8] We have now observed the Kondo effect in four SETs. All the data presented in this Letter are from a single SET nominally identical to, but distinct from, that discussed in [6].

- [9] A. C. Hewson, *The Kondo problem to heavy fermions, Cambridge Studies in Magnetism* (Cambridge University Press, Cambridge, 1993).
- [10] P. Nozières, Journal of Low Temperature Physics **17**, 31 (1974).
- [11] J. Kondo, in *Solid State Physics*, edited by H. Ehrenreich and D. Turnbull (Academic Press, New York, 1964), Vol. 23, p. 183.
- [12] D. R. Hamann, Physical Review **158**, 570 (1967).
- [13] T. A. Costi and A. C. Hewson, Journal of Physics: Cond. Mat. **6**, 2519 (1994).
- [14] In the latter case, a single-impurity picture is incomplete: inter-impurity interactions must also play a major role.
- [15] C. M. Varma, Rev. Mod. Phys. **48**, 219 (1976).
- [16] N. E. Bickers, Physical Review Letters **54**, 230 (1985).
- [17] F. D. M. Haldane, Physical Review Letters **40**, 416 (1978).
- [18] E. B. Foxman *et al.*, Physical Review B **50**, 14193 (1994).
- [19] Inoshita *et al.* [20] have proposed that Kondo temperatures in quantum dots should be enhanced by orders of magnitude if the quantized level spacing is small enough for several levels to participate in equilibrium transport. We do not see such a large enhancement, however we do observe satellites of the Kondo peak in differential conductance at bias  $V_{ds} \approx \pm \Delta\epsilon/2$ , as predicted for multilevel transport [20]. These results will be discussed in detail elsewhere.
- [20] T. Inoshita, Y. Kuramoto, and H. Sakaki, Superlattices and Microstructures **22**, 75 (1997).
- [21] There is no zero-bias peak in differential conductance in this region, demonstrating that the extra conductance is *not* caused by the Kondo effect here.
- [22] When  $-\tilde{\epsilon}_0 \gtrsim 2$  or  $-\tilde{\epsilon}_0 \lesssim 5.5$ , the measured  $T_K$  and  $G_0$  sharply decrease below their predicted values. This could be caused by an unintentional ac bias  $V_{ac}$  applied across the SET. Such a bias has often been known to raise the effective temperature of small electron systems. Here, it could have an even more drastic effect on the Kondo resonance, and hence on the conductance, at these values of  $\tilde{\epsilon}$ , for which  $V_{ac} \gtrsim T_K$ .

Figures printed separately:

FIG. 1.

FIG. 2.

FIG. 3.

FIG. 4.

FIG. 5.

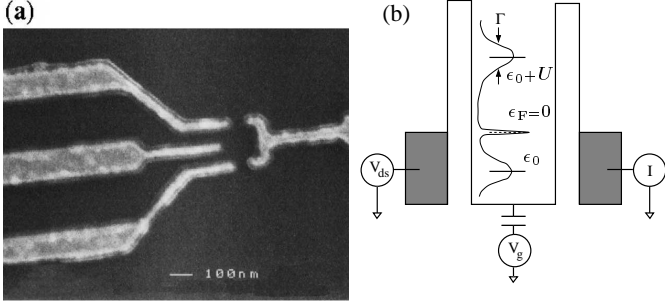


FIG. 1. (a) Electron micrograph of the SET. The lithographic diameter of the gate-enclosed central region is 150 nm. (b) Schematic energy diagram of the SET, showing an electron droplet separated by tunnel barriers from conducting leads. Since the number of electrons in the droplet is odd, the (inset) local density of states exhibits a sharp Kondo resonance at the Fermi level. The broad resonance at energy  $\epsilon_0$  represents a transition from  $n_d = 0$  to  $n_d = 1$ , while the one at  $\epsilon_0 + U$  corresponds to a transition from  $n_d = 1$  to  $n_d = 2$ .

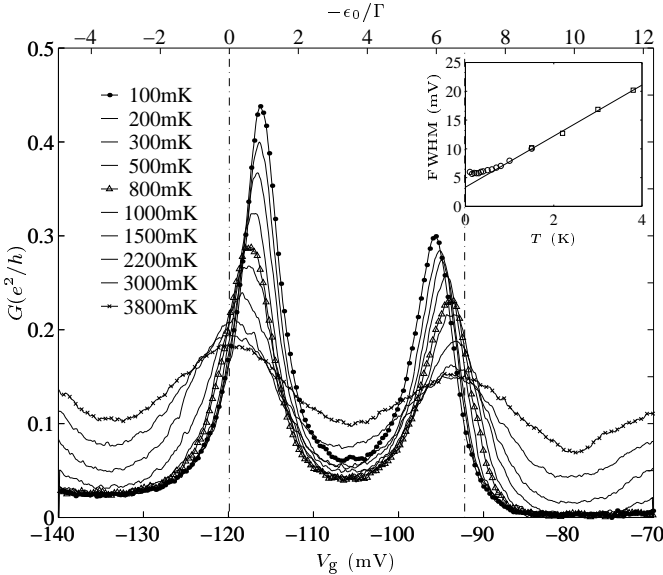


FIG. 2. Conductance versus plunger gate voltage  $V_g$  at various temperatures. The localized-state energy  $\epsilon_0 = \alpha V_g + \text{constant}$ . The vertical dashed lines mark gate voltages at which two charge states are degenerate (i.e.  $\epsilon_0 = 0$  or  $\epsilon_0 + U = 0$ ) based on the analysis in Figs. 5 (a),(b). Between the dashed lines the charge state of the site is odd, as portrayed in Fig. 1, and the Kondo effect enhances conductance. Inset: Linear temperature dependence of peak width extrapolated back to  $T = 0$  to extract  $\Gamma = 295 \pm 20 \mu\text{eV}$ . The slope of the same temperature-dependence gives the constant of proportionality  $\alpha = 0.069 \pm 0.0015$  between  $\epsilon_0$  and  $V_g$  [18].

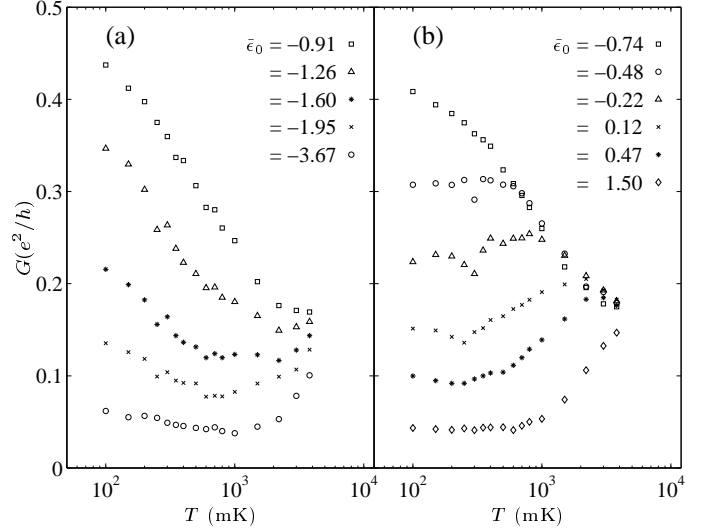


FIG. 3. Conductance versus temperature for various values of  $\epsilon_0$  on the right side (a) and left side (b) of the left-hand peak in Fig. 2.

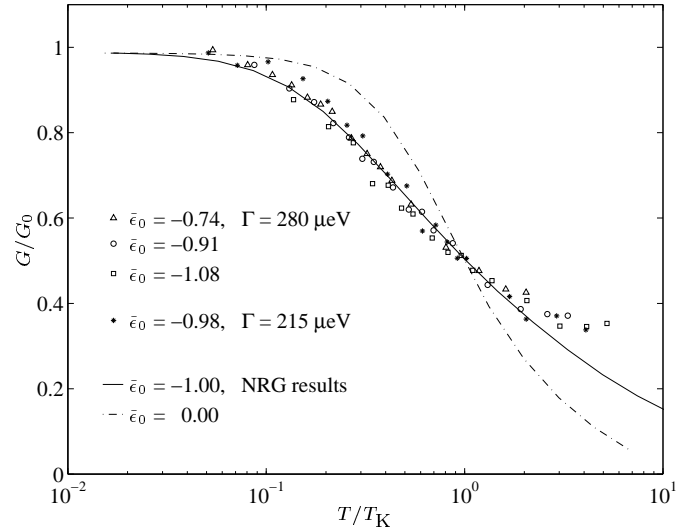


FIG. 4. The normalized conductance  $\tilde{G} \equiv G/G_0$  is a universal function of  $\tilde{T} \equiv T/T_K$ , independent of both  $\tilde{\epsilon}_0$  and  $\Gamma$ , in the Kondo regime, but depends on  $\tilde{\epsilon}_0$  in the mixed-valence regime. Scaled conductance data for  $\tilde{\epsilon}_0 \approx -1$  are compared with NRG calculations [13] for Kondo (solid line) and mixed-valence (dashed line) regimes. The stronger temperature dependence in the mixed-valence regime is qualitatively similar to the behavior for  $\tilde{\epsilon}_0 = -0.48$  in Fig. 3b.

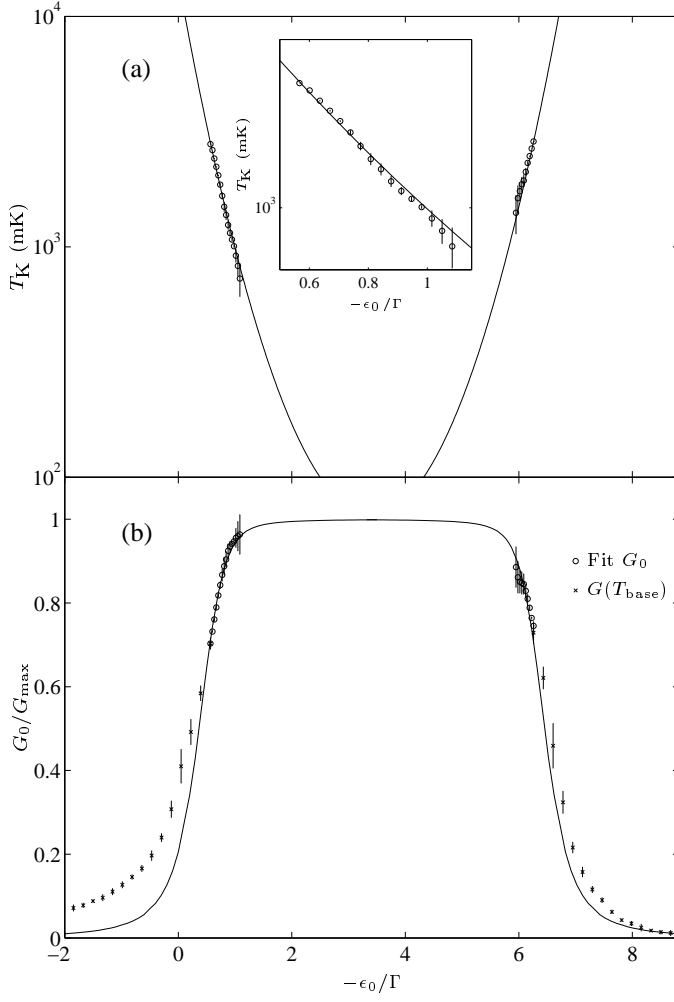


FIG. 5. (a) Fit values of  $T_K$  for data like those in Fig. 3 for a range of values of  $\epsilon_0$  [22]. The dependence of  $T_K$  on  $\epsilon_0$  is well-described by Eq. 1 (solid line). Inset: Expanded view of the left side of the figure, showing the quality of the fit. (b) Values of  $G_0$  extracted from data like those in Fig. 3 at a range of  $\epsilon_0$ . Solid line:  $G_0(\epsilon_0)$  predicted by Wingreen and Meir [4].  $G_{\max} = 0.49e^2/h$  for the left peak, and  $0.37e^2/h$  for the right peak.